Origin of Dark Current and Detailed Description of Organic Photodiode Operation Under Different Illumination Intensities

A. H. Fallahpour, S. Kienitz, and P. Lugli

Abstract—**Solution-processed organic-based photodetectors (OPDs) provide the opportunity to develop innovative, low cost, and large-area imaging technologies for industrial applications. However, compared to inorganic-based photodetectors, OPD devices have shown noticeably higher dark current and relatively lower sensitivity which is critical when the sensor needs to detect signals under low illumination intensities. Thus, to improve the design of OPDs, it is very important to know how opto-electrical response of the device is limited under the influences of structure, contact, and material layer properties. To analyze such limits, we employ a drift-diffusion approach to simulate a well-known and well-reproducible organic-based photodiode structure. Good agreement between current–voltage characteristics of the simulated result and experimental measurements under different illumination intensities confirms the presence of the traps is the origin of the high dark current in OPD devices. In addition, it is shown that traps have a dominant influence on the current–voltage characteristics of the device at low intensities, critical issue in several applications such as indirect X-ray detection technology. Based on this paper, to enhance OPD device performance operating in low intensities, it is recommended to put effort into processing (designing) a trap-free structure (material), rather than improving the material layer, structure, and contact properties.**

Index Terms—**Dark current, modeling and simulation, organic photodiode, trap state.**

I. INTRODUCTION

ORGANIC semiconductor devices have attracted great interest and are the center of attention as a promising alternative to inorganic-based devices. Organic semiconductors combine the mechanical advantage of polymers with the electronic advantages of semiconducting materials [1]. These unique properties, along with possibility of tailoring the opto-electrical properties of organic materials, allow inexpensive, robust, flexible, and large-area electronic devices to be developed [2], [3]. In particular, the photoconductive properties of organic-based photodetectors (OPDs) allow the development of innovative imaging technologies for industrial, security, and healthcare applications [4], [5].

In principle, OPDs have a similar structure as organic-based solar cells (OSCs); the difference lies in their mode of operation. In the case of photovoltaic cells, the interest is limited to high-intensity applications to harvest light across the solar spectrum, whereas sensitivity and signal detection are the main issues for OPD devices. Similar to OSCs, the key OPD parameters such as photo/dark current are related to the complex relationship between light absorption, charge transport, and free-carrier losses and extraction. Such physical processes are still under debate depending on the organic material structure, the morphology of the bulk-heterojunction layer, and the operation mode/condition of the device.

Despite the opto-electrical properties of organic-based solar cells having been well studied, the device characteristics and dominant losses mechanism of OPDs under dark and low light intensities are still lacking. In particular, OPD devices have shown considerably higher dark current (I_d) and lower sensitivity compared to inorganic-based photodetectors, which is significant when the sensor needs to detect signals at low intensities. In particular, to achieve high signal-to-noise ratios, the dark current should be minimized in order to improve fundamental aspects of the OPD like the power consumption, efficiency of signal detection, and the effectiveness of photocurrent readout process which is very significant in low illumination intensities. It has been shown experimentally that an investigation of blocking layers [6] and thick photoactive absorbers [7] can effectively suppress the dark current. While employing a blocking layer reduces the dark current to some extent [8], the thick absorber reduces the external quantum efficiency (EQE) of the OPD significantly. Low EQE is challenging for the device operates at low intensities (e.g., indirect X-ray detectors). Thus, in order to optimize the OPD performance proficiently, one important aspect that requires particular attention is to understand the origin and nature of high dark current and the dominant losses mechanism of the device under low illumination intensities.

In this paper, to provide a clear understanding of OPD performance limits, we developed a comprehensive model that gives the correct description of the device operation under various light illumination intensities. First, we investigate a macroscopic model based on the theory of organic solar cell device physics, and then by comparing the simulated result

This article has been accepted for inclusion in a future issue of this journal. Content is final as presented, with the exception of pagination.

2   IEEE TRANSACTIONS ON ELECTRON DEVICES
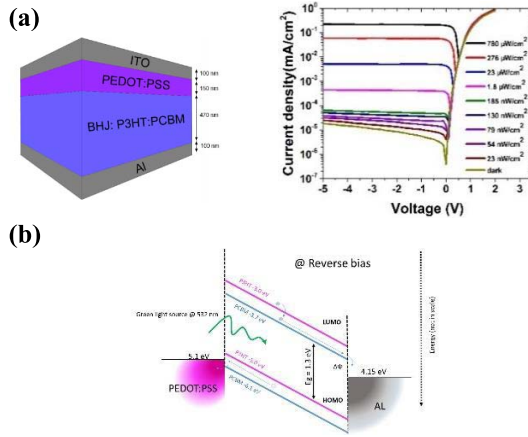

(a)

(b)

Fig. 1. (a) Schematic of the OPD layer structure and corresponding J–V characteristics under different green light intensities [12]. (b) Band diagram representation of the reference OPD structure.

with experimental measurements, we improved and validated the model for OPD devices. By performing several sets of simulations over the main physical parameters and inspecting the deviation of opto-electrical response of OPDs from measurement, we have finally identified the importance of device structure optimization, the modification of organic semiconductor material properties, and the design and synthesis of trap-free structure toward enhanced device performance.

II. MODEL DESCRIPTION

Simulation of semiconductor devices can be performed at different scales of abstraction, from the equivalent-circuit model to the Monte Carlo simulation where charge carrier interaction and transport are described by rate equations [9]. The former model introduces a high level of abstraction where effective parameters are investigated rather than reliable physical processes and the latter cannot be applied for practical device dimensions as it requires considerable computational cost and several input parameters that cannot be derived by measurements. Thus, both models introduce specific limits to simulate an entire set of current–voltage characteristics of the device. In this paper, the drift-diffusion model, which offers a good trade-off between physical depths and computational cost, is investigated. Since the drift-diffusion model has been widely described in literature [10], we neglect to duplicate its mathematical description here. Detailed description of our modeling approach can be found in [11].

III. DEVICE ARCHITECTURE, EXPERIMENTAL MEASUREMENT, AND SIMULATION PROCESS

As a reference, we analyze the opto-electrical characteristics of a well-reproducible and standard device structure; Indium thin oxide/poly-3,4- ethylenedioxythiophene: poly (styrenesulfonate) (PEDOT:PSS)/poly(3-ethylenedioxy)(P3HT) blended with [6,6]-phenyl C61 butyric acid methyl ester(PC$_{60}$ BM)/ Aluminum(Al). Fig. 1 shows schematically the layer structure and measured current–voltage characteristics of the reference OPD in the dark and under various monochromatic green light

TABLE I
INPUT PARAMETERS FOR SIMULATION

Description	Parameter	Value	Ref.
Light wavelength	λ	532 nm	
Absorber Thickness	L	470 nm	
Cathode work-function	Φ_{cath}	- 4.15	[13]
Anode work-function	Φ_{ano}	-5.1	[14]
HOMO (P3HT)	E_H	-5.0 eV	[15-17]
LUMO (PC$_{60}$BM)	E_L	-3.7 eV	[15-17]
Electron mobility	μ_e	2×10^{-3} cm^2/V.s	[18]
Hole mobility	μ_h	10^{-4} cm^2/V.s	[19, 20]
Permittivity	ε	3.2	
Recombination factor		1.26×10^{-9} cm^3/s	

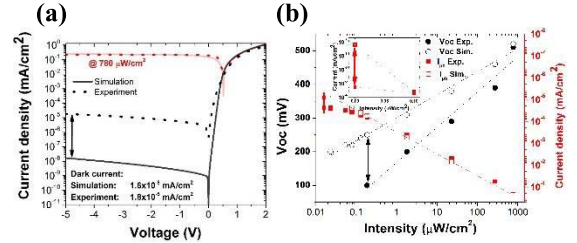**(a)**   **(b)**

Fig. 2. (a) Good agreement between J–V characteristics of simulation and experiment for high illumination intensities. (b) Significant difference between simulated result and measurement for the V_{oc} dark-and photo-current under low illumination intensities.

intensities [12]. The device shows a good diode behavior with a dark current value of about 1.8×10^{-5} mA/cm^2 at -5 V and a rectification ratio of about 4.4×10^4 at $+2/-5$ V. As a step toward quantifying the effect of physical parameters and material properties, first we evaluated the agreement between experimental results and simulations with regards to the J–V characteristics of the cell under high illumination intensities. Despite the physical parameters of organic polymers not being as precise as inorganic semiconductors, those of blended P3HT:PC60BM have frequently been reported to confined ranges. The input parameters for our simulations were taken from experimental measurements in the literature are summarized in Table I.

Starting with the parameters in Table I, we simulate the device in 2-D, where the mesh setting to 20 nm for active area and 5 nm at the interfaces ensured reasonable running times and accurate results. As expected [Fig. 2(a)], by considering the physics of solar cells, good agreement between the calculated J–V characteristics and experimental measurement was observed for the device illuminated under Sun [(1.5 AM (100 mW/cm^2)] and moderate green light illumination intensities (780 μW/cm^2). However, the simulated result fails to reproduce a reliable opto-electrical response of the reference OPD at dark and low intensities. This is shown in Fig. 2(b), where the simulated characteristics of the device under different illumination intensities are compared to the measurements. As shown, beside orders of magnitude differences in dark current [inset of Fig. 2(b)], the simulated photocurrent starts to deviate from experimental measurements at low illumination intensities (<1 μW/cm^2). In addition, even the open-circuit voltage (V_{oc}) of the simulated cell matches at high illumination

This article has been accepted for inclusion in a future issue of this journal. Content is final as presented, with the exception of pagination.

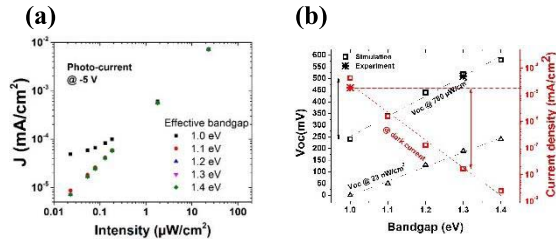FALLAHPOUR *et al.*: ORIGIN OF DARK CURRENT AND DETAILED DESCRIPTION

3

Fig. 3. (a) Systematic variation of the effective bandgap marginally influences on the photocurrent. (b) Simulated dark currents fits with the measurement for the nominal effective band gap of ~1 eV, however, the calculated V_{oc} deviated significantly from the measurement, especially at high illumination intensities (see horizontal dashed guideline from experimental measurement).

Fig. 4. (a) Increasing barrier high results in higher Id and lower forward bias current as a result of minority and majority charge injection into photoactive layer. (b) Figure of merits (I_d, V_{oc}, and I_f) disagreement between simulated and measurement for different barrier highs.

intensities; at low illumination intensities, considerably lower V_{oc} is calculated compared to the measurement. V_{oc} represents the maximum voltage that the device can provide to an external circuit in photovoltaic mode. V_{oc} is one of the most important parameters in which no net current exists at any point within the device. In V_{oc} carrier generation and losses exactly counterbalance each other, where the accumulation of photo-generated carriers constituting a potential difference that cancels out the built-in potential. In such conditions, different physical processes and material properties could influence the V_{oc} of the device [21]; thus, it is very important to have a precise approximation of V_{oc} of the device under different illumination intensities.

IV. RESULTS AND DISCUSSION

The thermally generated carrier, charge injection from the contact, recombination mechanism and defects in the bulk and interfaces of photoactive layer, all highly influence the characteristics of organic photodiodes. In order to understand the origin of high leakage current and significant deviation of calculated V_{oc}, I_d, and I_{ph} from the measurement, we perform several sets of simulations by varying the electrical properties of the layer structure and the physical parameters in their nominal value.

As known, the main drawback of the narrow bandgap semiconducting material is the increase of thermally generated dark current which could be the source of high leakage current in the OPD. Thus, to analyze the effect of bandgap on the device characteristics, the effective bandgap [Lowest unoccupied molecular orbital (LUMO) of the acceptor ($PC_{60}BM$) and highest occupied molecular orbital (HOMO) of the donor (P3HT)] of the device photoactive layer were systematically varied close to the reported values in literature. As shown in Fig. 3, while the variation of photocurrent under different illumination intensities is very limited for the lower bandgaps, the deviation of calculated V_{oc} and dark current is more pronounced.

The simulated V_{oc} fits very well with the experimental results for the nominal effective bandgap [~1.3 eV in Fig. 3(b)]; however, under such conditions, the dark current [as well as the photocurrent at low intensity: Fig. 2(b)] is significantly underestimated. On the other hand, for low bandgaps [Fig. 3(b)], the dark current increases as extra thermally generated carrier within the depletion region swept out toward the contact and act as leakage current. Even for the
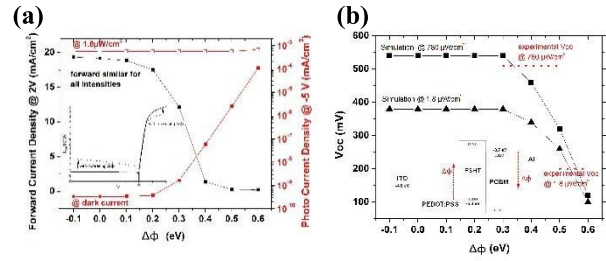
bandgaps lower than 1 eV the simulated dark current matches experimental measurements, but in such condition, the open circuit voltage is shifted to lesser values that do not follow experimental measurements [e.g., 780 μW/cm^2 in Fig. 3(b)].

Comparing the simulated result to the experiment, we can conclude that the effective band gap of the material is unlikely the origin of such a high dark current, as the simulation does not agree with the device characteristics of the reference experiment (and the literature) under different illumination intensities.

Next, to investigate the effect of charge injection/extraction at the semiconductor interface, the work function of the contacts and the barrier high varied smoothly, and the simulated result compared to the figure of merit of the reference device. The contact-originated dark current is the consequence of charge injection from the device contact, where electron (hole) injection takes place from the hole (electron) collecting electrode of the device to the photoactive layer. This is the reason why the electron (hole) blocking layer is commonly inserted between the photoactive layer and the anode (cathode) to suppressed leakage current from anode to the photoactive layer [6]. In our device configuration, the energetic barrier for the hole (electron) injection is the difference between work function of Al (PEDOT) with HOMO (LUMO) of $PC_{60}BM$ (P3HT). The simulated characteristics of OPD for different barrier high and on the basis of Mott–Schottky theory are shown in Fig. 4. A decrease in the apparent barrier height significantly influences the injection and extraction of the charge carriers. This effect is highlighted for the current density in reverse and forward biases. In reverse bias, reducing the barrier high enhances the hole (electron) injection from the Al cathode (PEDOT anode) in to the photoactive layer, which in turn increases the dark current.

In addition, at relatively high reverse bias, the polymer HOMO (LUMO) level bends upward (downward) and enables the tunneling of electrons from the cathode (anode) through the energy barrier to the active layer. Thus, the lower the cathode work function, the higher the tunneling probability and carrier injection.

As shown in Fig. 4(a), at forward bias (+2 V), the charges can be efficiently injected into the blend for low injection barriers and it is minimized for relatively high $\Delta\Phi$. This is due to the fact that a lower fraction of majority carriers can pass the potential barrier to inject into the photoactive layer. For all injection barriers, the consistent photocurrent with marginal

This article has been accepted for inclusion in a future issue of this journal. Content is final as presented, with the exception of pagination.

4   IEEE TRANSACTIONS ON ELECTRON DEVICES

deviation from the experiments is observed. In contrast, the estimated dark current density value was far from the measurement for low $\Delta\Phi$ and it dramatically increased for relatively high $\Delta\Phi$. As is depicted in Fig. 4, the simulated barrier high that shows comparable dark current with the experimental measurements strongly deviates (by 0.3 eV) from the typical work function of our device contacts. However, assuming the existence of such a barrier, the deviation of current density and $V_{\rm oc}$ from measurement is still considerably high for different illumination intensities.

Inconsistency between measurements and simulations also holds for $V_{\rm oc}$ of the device under low and high illumination intensities. As shown in Fig. 4(b), under low illumination intensities, the simulated $V_{\rm oc}$ fails to reproduce the measurements for both high and low $\Delta\Phi$. On the other hand, under high illumination intensities, consistent $V_{\rm oc}$ is reproduced for low barrier high, but for high $\Delta\Phi$ (where comparable Id with the experiment is observed), the simulated $V_{\rm oc}$ differed significantly from the measurement. Thus, disagreement under different operating conditions confirms contact behaviors and carrier injection from the contacts are likely not the origin of such deviation of dark current seen in the reference OPD.

Next, we analyze the effect of charge carrier recombination and losses mechanisms on the characteristics of the device. There is huge debate concerning the loss mechanisms and nature of the recombination process in organic bulk-heterojunction based devices. This is an important process because the charge carrier collection efficiency (and hence the current–voltage characteristics of the OPD) are related to the interplay between charge carrier extraction and recombination process. It is extensively shown the expected recombination mechanism in low-mobility materials is Langevin-type recombination, where the time of an electron and a hole finding each other defines the recombination rate. Experimentally it has been shown [22]–[24] that the Langevin rate, as a function of charge carrier mobility, only gives an approximate recombination rate. The precise recombination rate which is highly related to the internal morphology of the blended structure and the device process condition needs to be estimated with experimental measurement. Thus, we arbitrarily varied the recombination rate in our simulations to reproduce comparable dark current observed in device. The prefactor value (Fig. 5) that reproduces the experiment was unphysical (ß $\gg$ 1). In addition, considering such a huge recombination is an inappropriate assumption, since as shown in Fig. 5, the simulated $V_{\rm oc}$ (assuming such losses) as well as short-circuit current ($I_{\rm sc}$) is noticeably lower than the measurements. In particular, for low recombination rates (commonly investigated for OSCs); the dark current, and for relatively high recombination rate; both short circuit current (e.g., $I_{\rm sc} < 1$ mA/cm^2 for the Sun) and $V_{\rm oc}$ (especially under high intensities), deviates considerably from the measurements.

V. Traps as a Origin of High Dark Current

Inconsistency between measurement and simulated I_d, $I_{\rm ph}$, and $V_{\rm oc}$ under different illumination intensities confirms the

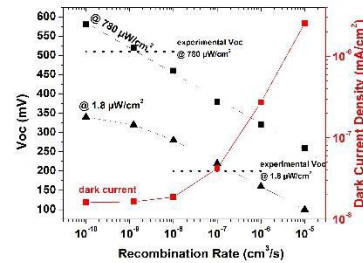Fig. 5.   Dark current increases and match with experiment for relatively high Langevin recombination rate (unphysical).Assuming such losses mechanism, still $V_{\rm oc}$ and $I_{\rm sc}$ (not shown) significantly deviated from measurement.
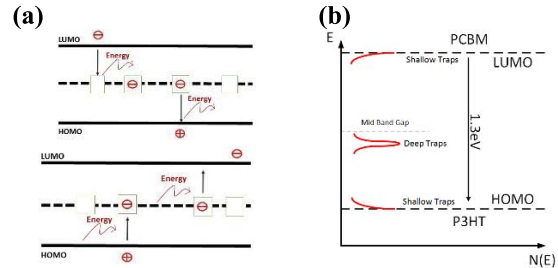

Fig. 6.   (a) Cartoon that conceptually illustrating recombination and generation processes through trap state. (b) Schematic representation of density of state of shallow and deep trap levels.

existence of extra losses mechanisms and presence of the traps in the device. Impurities, defects, surface states, dangling bonds, and localized stresses [25] can act as trapping centers in organic materials. Traps have extrinsic and intrinsic origins. Extrinsic traps originate from extrinsic defects, such as chemical impurities introduced during material synthesis, and exposure to oxygen or moisture etc. Intrinsic traps originate from intrinsic defects such as those arising from morphological disorder and amorphous nature of organic semiconductors.

Trap states are also distinguished into deep traps and shallow traps (Fig. 6). For instance, oxygen and moisture introducing shallow trap levels, where morphological ordering and air exposure strongly influence on deep trap concentration [25]. In practice, the influences of different trap states are mixed in blended organic semiconductors, thus, it is very challenging to precisely determine all the trap properties such as the densities, charges (positive, negative or neutral), types (donor-or acceptor-type) and kinds (interface or bulk) of the traps.

The exact identification and characterization of the origin of the traps in organic semiconductors are beyond the scope of this work. Instead, we investigate traps dynamics in our simulation in order to analyze their effect on the electrical response of OPD device. In particular, trap states significantly influence on carrier concentration, continuity equation, and transport mechanism of the OPD as a result of capture and emission of electrons from/into the HOMO and LUMO levels via trap states [see Fig. 6(a)].

As schematically shown in Fig. 6(b), it has been reported that both shallow and deep trap states present in the bandgap of P3HT:PC$_{60}$BM [25]. Thus, the charge transport model of the reference cell developed to include multiple trap dynamics. In this regard, both shallow and donor-like deep traps para-

This article has been accepted for inclusion in a future issue of this journal. Content is final as presented, with the exception of pagination.

FALLAHPOUR *et al.*: ORIGIN OF DARK CURRENT AND DETAILED DESCRIPTION
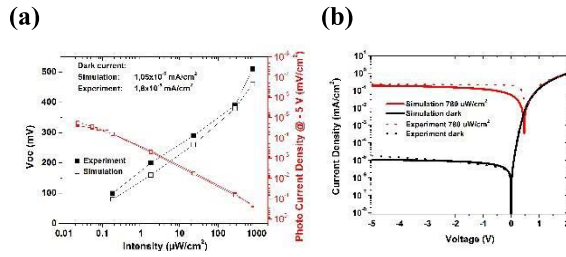5

(a)   **(b)**

Fig. 7. Implementing traps to the model results in an accurate simulation of the photodiode at high and low illuminations. (a) Shows that photocurrent and V_{oc} match the experimental OPD. (b) Illustrates the experimental and simulated *J–V* curve at two different illumination intensities.

TABLE II
SHALLOW AND DEEP TRAP PARAMETERS

Trap	Description	parameter
Deep	Distribution	Gaussian
	Offset from HOMO	550 meV
	Concentration (cm⁻³)	10^{15}
	Sigma of Energy Function	80 meV
Shallow	Distribution	Exponential
	Offset from HOMO	200 meV
	Concentration (cm⁻³)	10^{15}
	Sigma of Energy Function	80 meV

meters varied in their nominal reported value in the literature. The simulated result shows that, while the characteristic of the device for high illumination intensities was almost unaffected, the presence of traps hugely influences on the dark and photocurrent density of the OPD at low illumination intensities. In particular, the effect of deep traps is more pronounced and the dark current mostly controlled with high concentration of trap density that provide a coupled recombination/generation paths through the trap states. As verified with the simulated data shown in Fig. 7, with trap parameters close to those reported in the literature (Table II), the dark current, photocurrent, and V_{oc} become in agreement with the measurements for all illumination intensities. In particular, traps begin to make noticeable contributions to control photocurrent as well as the dark current at low intensities. The former is due to the defect density that provides coupled recombination paths through trap states, which increases the losses under illumination. The latter is due to the enhanced thermally generated carrier density (i.e., random thermal excitation causing an electron to jump from the LUMO to an unoccupied trap level, and then from this level to the HOMO level) that swept from the depletion region, and contributed to the dark current.

To conclude, comparing the simulated result with the experimental measurements suggest beyond the contact and organic material properties, trap states are the main source of the high dark current and low sensitivity in the OPDs operating at low illumination intensities. Therefore, to improve the performance of the OPDs operating in low illumination intensities, it is recommended to put effort into designing a trap-free material rather than optimizing the structure, contact and material layer properties.

VI. CONCLUSION

In this paper, to evaluate the origin of the high dark current and relatively poor sensitivity of OPDs, we systematically analyzed the effect of material layer properties and physical processes on the figures of merit (I_{ph}, I_d, I_f, and V_{oc}) of the device under different operating conditions. The model shows excellent agreement with experimental measurements under different illumination intensities and over the entire bias range only if traps are introduced. In particular, by separating out the different contributions of material and contact properties in our simulation, traps are shown to be responsible for the relatively high dark current and poor sensitivity in OPDs. In addition, it is shown depending on the trap and excess charge carrier (illumination intensity) densities, monomolecular losses (trap assisted losses) dominate at low illumination intensities, while bimolecular losses (Langevin type) dominate at high illumination intensities. The former is due to the defect density, while the latter is due to the quadratic dependence of losses on the charge carrier density. Ultimately, we suggest to further improve the electrical response of OPD devices operating under low illumination intensities (e.g., indirect X-ray photodetectors), the design and synthesis of trap-free materials are more important than the optimization of contact and organic material layer properties.

REFERENCES

[1] H. Dong, H. Zhu, Q. Meng, X. Gong, and W. Hu, "Organic photoresponse materials and devices," *Chem. Soc. Rev.*, vol. 41, pp. 1754–1808, Sep. 2012.

[2] L. Lu, T. Zheng, Q. Wu, A. M. Schneider, D. Zhao, and L. Yu, "Recent advances in bulk heterojunction polymer solar cells," *Chem. Rev.*, vol. 115, no. 23, pp. 12666–12731, 2015.

[3] H. Zhang *et al.*, "Transparent organic photodetector using a near-infrared absorbing cyanine dye," *Sci. Rep.*, vol. 5, p. 9439, Mar. 2015.

[4] R. D. Jansen-van Vuuren, A. Armin, A. K. Pandey, P. L. Burn, and P. Meredith, "Organic photodiodes: The future of full color detection and image sensing," *Adv. Mater.*, vol. 28, pp. 4766–4802, Jun. 2016.

[5] P. Büchele *et al.*, "X-ray imaging with scintillator-sensitized hybrid organic photodetectors," *Nat. Photon.*, vol. 9, pp. 843–848, Mar. 2015.

[6] X. Gong, M.-H. Tong, S. H. Park, M. Liu, A. Jen, and A. J. Heeger, "Semiconducting polymer photodetectors with electron and hole blocking layers: High detectivity in the near-infrared," *Sensors*, vol. 10, p. 6488, Apr. 2010.

[7] A. Armin, M. Hambsch, I. K. Kim, P. L. Burn, P. Meredith, and E. B. Namdas, "Thick junction broadband organic photodiodes," *Laser Photon. Rev.*, vol. 8, pp. 924–932, Jan. 2014.

[8] S. Yoon, J. Cho, K. M. Sim, J. Ha, and D. S. Chung, "Low dark current inverted organic photodiodes using anionic polyelectrolyte as a cathode interlayer," *Appl. Phys. Lett.*, vol. 110, p. 083301, Sep. 2017.

[9] T. Albes, P. Lugli, and A. Gagliardi, "Investigation of the blend morphology in bulk-heterojunction organic solar cells," *IEEE Trans. Nanotechnol.*, vol. 15, no. 2, pp. 281–288, Mar. 2016.

[10] L. J. A. Koster, E. C. P. Smits, V. D. Mihailetchi, and P. W. M. Blom, "Device model for the operation of polymer/fullerene bulk heterojunction solar cells," *Phys. Rev. B, Condens. Matter*, vol. 72, p. 085205, Jun. 2005.

[11] A. H. Fallahpour *et al.*, "Modeling and simulation of energetically disordered organic solar cells," *J. Appl. Phys.*, vol. 116, p. 184502, Sep. 2014.

This article has been accepted for inclusion in a future issue of this journal. Content is final as presented, with the exception of pagination.

6   IEEE TRANSACTIONS ON ELECTRON DEVICES

[12] F. Arca, "Organic photodiodes for industrial sensing and medical," Ph.D. dissertation, Dept. Inst. Nanoelectron., München, Germany, Technische Universität München, 2013, p. 128.

[13] T. M. Brown, G. M. Lazzerini, L. J. Parrott, V. Bodrozic, L. Bürgi, and F. Cacialli, "Time dependence and freezing-in of the electrode oxygen plasma-induced work function enhancement in polymer semiconductor heterostructures," *Organic Electron.*, vol. 12, pp. 623–633, Apr. 2011.

[14] T. M. Brown, J. S. Kim, R. H. Friend, F. Cacialli, R. Daik, and W. J. Feast, "Built-in field electroabsorption spectroscopy of polymer light-emitting diodes incorporating a doped poly(3,4-ethylene dioxythiophene) hole injection layer," *Appl. Phys. Lett.*, vol. 75, pp. 1679–1681, Sep. 1999.

[15] M. C. Scharber *et al.*, "Design rules for donors in bulk-heterojunction solar cells-towards 10% energy-conversion efficiency," *Adv. Mater.*, vol. 18, pp. 789–794, Apr. 2006.

[16] J. Y. Kim *et al.*, "New architecture for high-efficiency polymer photovoltaic cells using solution-based titanium oxide as an optical spacer," *Adv. Mater.*, vol. 18, no. 5, pp. 572–576, 2006.

[17] W.-H. Baek, H. Yang, T.-S. Yoon, C. J. Kang, H. H. Lee, and Y.-S. Kim, "Effect of P3HT:PCBM concentration in solvent on performances of organic solar cells," *Solar Energy Mater. Solar Cells*, vol. 93, pp. 1263–1267, Sep. 2009.

[18] G. Garcia-Belmonte, A. Munar, E. M. Barea, J. Bisquert, I. Ugarte, and R. Pacios, "Charge carrier mobility and lifetime of organic bulk heterojunctions analyzed by impedance spectroscopy," *Organic Electron.*, vol. 9, pp. 847–851, Apr. 2008.

[19] F. Torricelli, Z. M. Kovács-Vajna, and L. Colalongo, "The role of the density of states on the hole mobility of disordered organic semiconductors," *Organic Electron.*, vol. 10, pp. 1037–1040, Aug. 2009.

[20] C. Tanase, E. J. Meijer, P. W. M. Blom, and D. M. de Leeuw, "Unification of the hole transport in polymeric field-effect transistors and light-emitting diodes," *Phys. Rev. Lett.*, vol. 91, p. 216601, Nov. 2003.

[21] N. K. Elumalai and A. Uddin, "Open circuit voltage of organic solar cells: An in-depth review," *Energy Environ. Sci.*, vol. 9, pp. 391–410, 2016.

[22] A. Pivrikas *et al.*, "Bimolecular recombination coefficient as a sensitive testing parameter for low-mobility solar-cell materials," *Phys. Rev. Lett.*, vol. 94, p. 176806, May 2005.

[23] L. J. A. Koster, V. D. Mihailetchi, and P. W. M. Blom, "Bimolecular recombination in polymer/fullerene bulk heterojunction solar cells," *Appl. Phys. Lett.*, vol. 88, p. 052104, Apr. 2006.

[24] A. Pivrikas, H. Neugebauer, and N. S. Sariciftci, "Charge carrier lifetime and recombination in bulk heterojunction solar cells," *IEEE J. Sel. Topics Quantum Electron.*, vol. 16, no. 6, pp. 1746–1758, Jun. 2010.

[25] J. A. Carr and S. Chaudhary, "The identification, characterization and mitigation of defect states in organic photovoltaic devices: A review and outlook," *Energy Environ. Sci.*, vol. 6, pp. 3414–3438, Apr. 2013.